PERGAMON

Journal of Structural Geology 25 (2003) 1097–1106

JOURNAL OF STRUCTURAL GEOLOGY

www.elsevier.com/locate/jsg

# Role of nappe boundaries in subduction-related regional deformation: spatial variation of meso- and microstructures in the Seba eclogite unit, the Sambagawa belt, SW Japan

Mutsuki Aoya*, Simon R. Wallis

*Department of Earth and Planetary Sciences, Graduate School of Environmental Studies, Nagoya University, Nagoya 464-8601, Japan*

Received 28 November 2001; accepted 16 August 2002

**Abstract**

The Seba eclogite unit of the Sambagawa high-*P*/*T* metamorphic belt has a kilometre-scale synformal structure and its base is the boundary between an overlying eclogite nappe and an underlying non-eclogitic nappe. The formation of the nappe boundary is related to a phase of strong penetrative ductile deformation ($D_A$). Spatial variations of meso- and microstructures of schistose eclogite in the Seba unit reveal that there is (i) a decreasing intensity of $D_A$, and (ii) a time-dependent widening of the $D_A$ shear zone, away from the nappe boundary. These features indicate that the nappe boundary behaved as a core zone during the $D_A$ phase and, furthermore, that development of the regional deformation, $D_A$, is strongly controlled by the presence of the nappe boundary. A new model is proposed where each phase of regional deformation in subduction-type metamorphic belts is related to ancient activity of a particular nappe boundary. In this model a single phase of deformation may be related to exhumation in one nappe and subduction in an adjacent one.


*Keywords:* Deformation; Eclogite; Microstructure; Nappe; Sambagawa belt

## 1. Introduction

Regional metamorphic belts found in the internal parts of convergent orogens are characterised by polyphase ductile deformation (e.g. Passchier and Trouw, 1996). Discrete deformation phases are recognised by the presence of refolded folds and foliations crosscut by newer deformational fabrics. In many cases individual deformation phases can be traced throughout large parts of particular orogens and the identification of such regionally developed deformation phases (structural analysis) is widely used by structural geologists to establish a framework for correlating geological events on scales of whole orogens. A second reason for performing structural analysis is that regionally developed phases of penetrative deformation reflect large-scale crustal flow and, therefore, have tectonic significance. A number of workers have documented cases where steeply dipping tectonic fabrics developed during plate convergence and horizontal shortening are overprinted by deformation associated with flat-lying fabrics related to extension and vertical thinning (e.g. Burg et al., 1992; Froitzheim, 1992; Platt et al., 1998). A second example is the regional development of a phase of back-folding and associated cleavage in the European Alps that can be related to collision and thickening (e.g. Roeder, 1973). In many regions, however, there are far more phases of ductile deformation than can easily be accommodated by such tectonic interpretations. One possible explanation is that the multiple phases of folding and foliation formation develop during a single phase of progressive non-coaxial shear (e.g. Quinquis et al., 1978). In this contribution we suggest an alternative model, where individual phases of deformation may be related to movement along a major nappe boundary. In our proposed model a single phase of deformation may be related to exhumation in one nappe and subduction in an adjacent one.

## 2. Structural and metamorphic back ground

The Sambagawa high-*P*/*T* metamorphic belt of SW Japan (Fig. 1) formed in a typical subduction-zone setting during a single subduction-related metamorphic episode of

* Corresponding author. Tel.: +81-52-789-3004; fax: +81-52-789-3005.
*E-mail address:* aoya@mbox.media.nagoya-u.ac.jp (M. Aoya).

0191-8141/03/$ - see front matter © 2002 Elsevier Science Ltd. All rights reserved.
PII: S0191-8141(02)00147-5

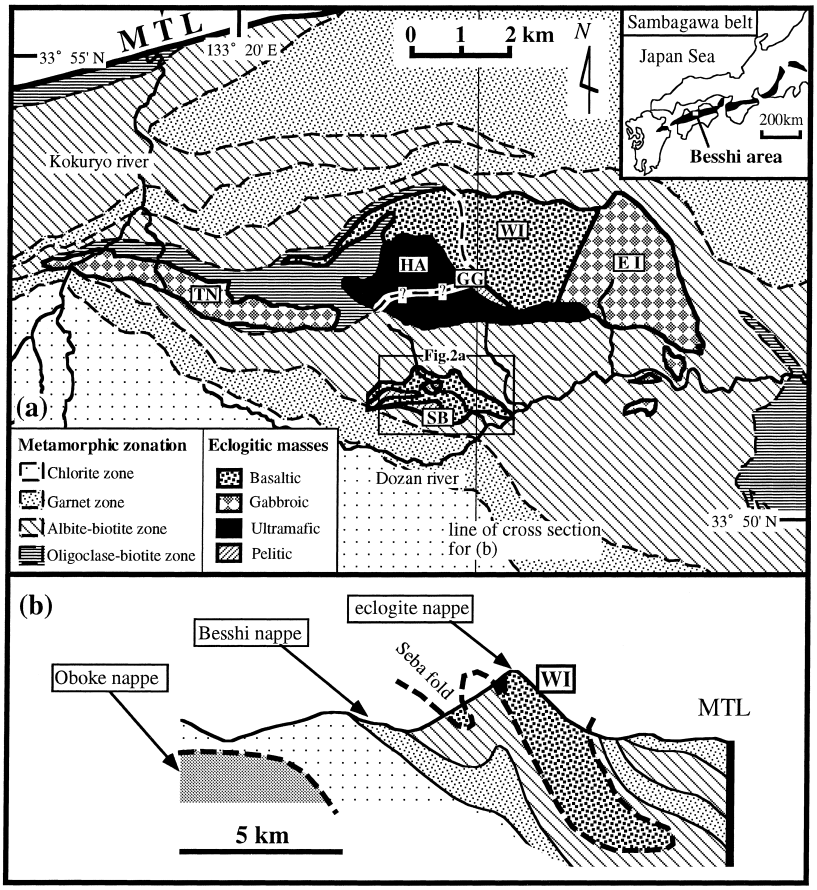


Fig. 1. (a) Geological map of the Besshi area showing localities of eclogitic masses (after Takasu, 1989; Enami, 1996; Wallis and Aoya, 2000) and metamorphic zonation for non-eclogitic schists (Higashino, 1990). (b) Schematic N–S cross-section along the line shown in (a) (after Wallis and Aoya, 2000). MTL = Median tectonic line; TN = Tonaru mass; HA = Higashi Akaishi mass; GG = Gongen mass; WI = Western Iratsu mass; EI = Eastern Iratsu mass; SB = Seba unit.

the late Cretaceous period (e.g. Banno and Nakajima, 1992). Based on petrological, geochronological, and structural data, it is generally accepted that two major non-eclogitic thrust sheets or nappes can be defined in the Sambagawa belt (e.g. Takasu et al., 1994; Wallis, 1998): the Besshi and Oboke nappes (Fig. 1). Both these nappes are considered to have behaved as coherent units during subduction and subsequent exhumation, because they show internally consistent peak metamorphic conditions, they show similar ranges of K–Ar and Ar–Ar age data and they display the same sets of penetrative deformation stages. In addition, it has recently been proposed that the eclogite-bearing masses form a composite third nappe, the eclogite nappe, and this can be viewed as the highest grade unit within the Sambagawa belt (e.g. Wallis and Aoya, 2000; Fig. 1b). In most areas in the Sambagawa belt, however, the positions of the nappe boundaries have not been clearly determined in the field and it is still unclear what deformational effects these nappe boundaries may have exerted on the rocks around them. One exception is the area around the Seba unit (Fig. 2) where it is possible to discuss in detail the deformational development of the nappe boundary because: (i) the position of the tectonic boundary between the eclogitic Seba unit and the non-eclogitic Besshi nappe has been well constrained (Wallis and Aoya, 2000; Fig. 2); (ii) the large-scale structure of the region has been determined (Aoya, 2002; Fig. 2c); and (iii) the particular deformation stage related to the formation of the nappe boundary has been identified as $D_A$ of Aoya and Wallis (1999) (Fig. 2b) by using a combination of structural and petrological analyses (Aoya, 2001). The last point implies that in the Seba unit consisting dominantly of basic schist (Fig. 2), the deformational evolution of the nappe boundary can be discussed by focusing on $D_A$ structures. The $D_A$ deformation is related to exhumation from the eclogite facies to the epidote amphibolite facies (Aoya, 2001) and is defined by a schistosity that contains a strong linear alignment of omphacite (Aoya and Wallis, 1999). Although its strength varies, the schistosity formed during $D_A$ ($S_A$) is observed throughout the Seba basic schist with the exception of the most internal part adjacent to the Seba metagabbro where $S_0$, an older schistosity formed during $D_0$ deformation, is preserved (Aoya, 2001; Fig. 3). The $S_A$ schistosity and the associated nappe boundary defining the base of the Seba unit are folded together by a later deformation stage, $D_B$, into a large-scale synform with the Seba unit at the highest structural levels (Aoya, 2002; Fig. 2c).

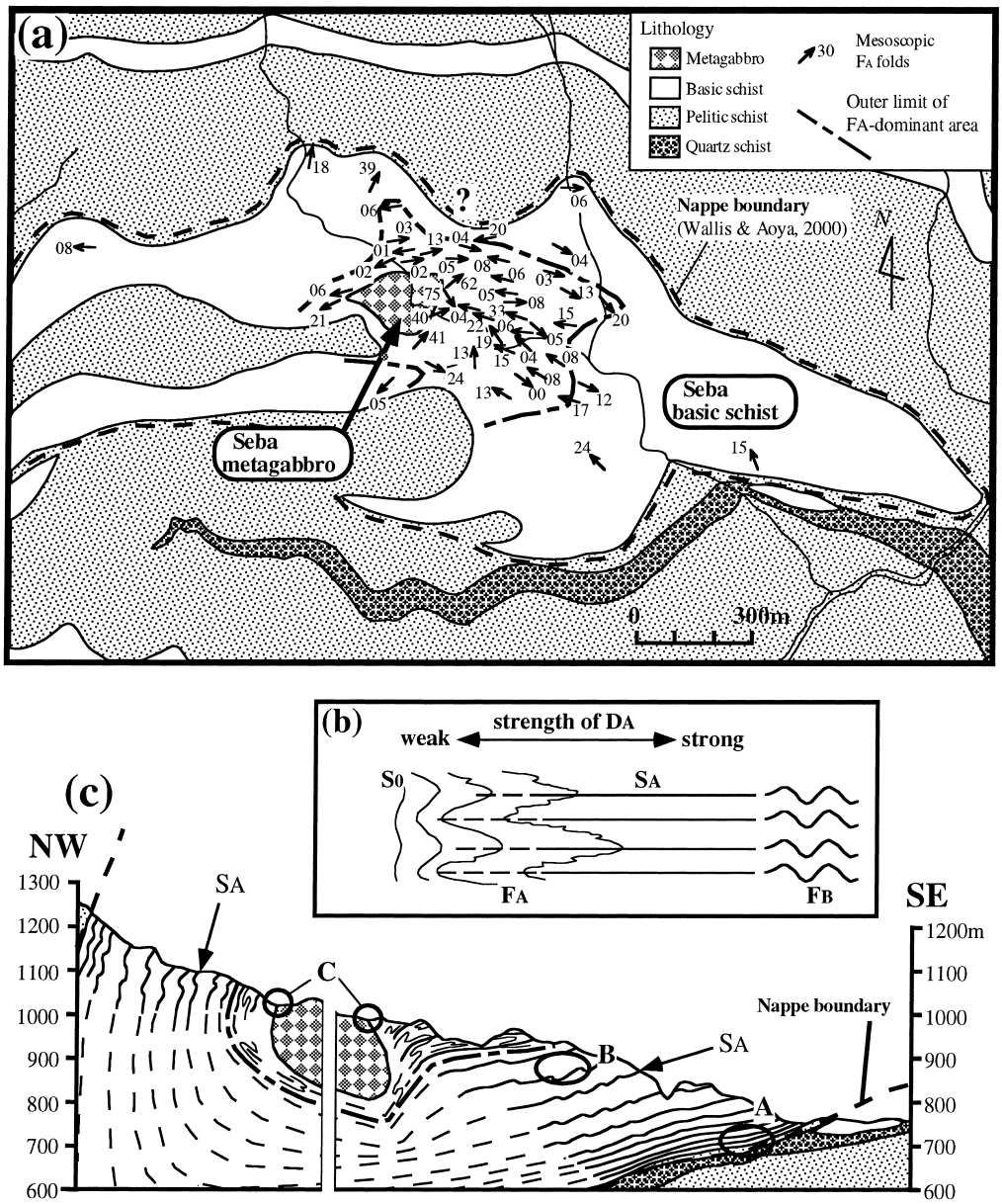


Fig. 2. (a) Geological map around the Seba eclogite unit showing distribution of mesoscopic $F_A$ folds. (b) Schematic illustration showing the relationships of mesostructures in the Seba basic schist. Three deformation stages, $D_0$, $D_A$ and $D_B$ in chronological order, are defined by Aoya and Wallis (1999). (c) Cross-sections along the lines shown in Fig. 3a. Structural position of localities A, B and C, where three types of microstructures of eclogitic garnet (Fig.5) are recognised, are also shown.

## 3. Decreasing strength of $D_A$ away from the nappe boundary

The Seba basic schist (Fig. 2a) is dominantly composed of micaceous garnet epidote amphibolite with a minor amount of eclogitic rocks with garnet + omphacite assemblages (e.g. Aoya, 2001). In the Seba basic schist, a gradual change in the strength of $D_A$ deformation can be recognised by changes in outcrop-scale $D_A$ structures from distinct $F_A$ folds that pass into tighter folds and eventually into regions where the old $S_0$ foliation is completely transposed and only a strongly developed $S_A$ schistosity is observed (Aoya and Wallis, 1999; Fig. 2b). In Aoya and Wallis (1999), this contrast in the nature of $D_A$ mesostructures is shown only for one particular cross-section. Recent field studies have developed this work and revealed the distribution of mesoscopic $F_A$ folds throughout the Seba basic schist (Fig. 2a). It is now evident that the $F_A$-dominant area is located in the central part of the Seba basic schist and is surrounded by a peripheral $S_A$-dominant area (Fig. 2a). This indicates that the region of low $D_A$ strain is located in the central part of the Seba basic schist.

In addition to the $D_A$ mesostructures, the microstructure of omphacite in eclogite samples can also be used as a qualitative indicator of the strength of $D_A$ (Fig. 3). Omphacite microstructure shows a gradual change from a

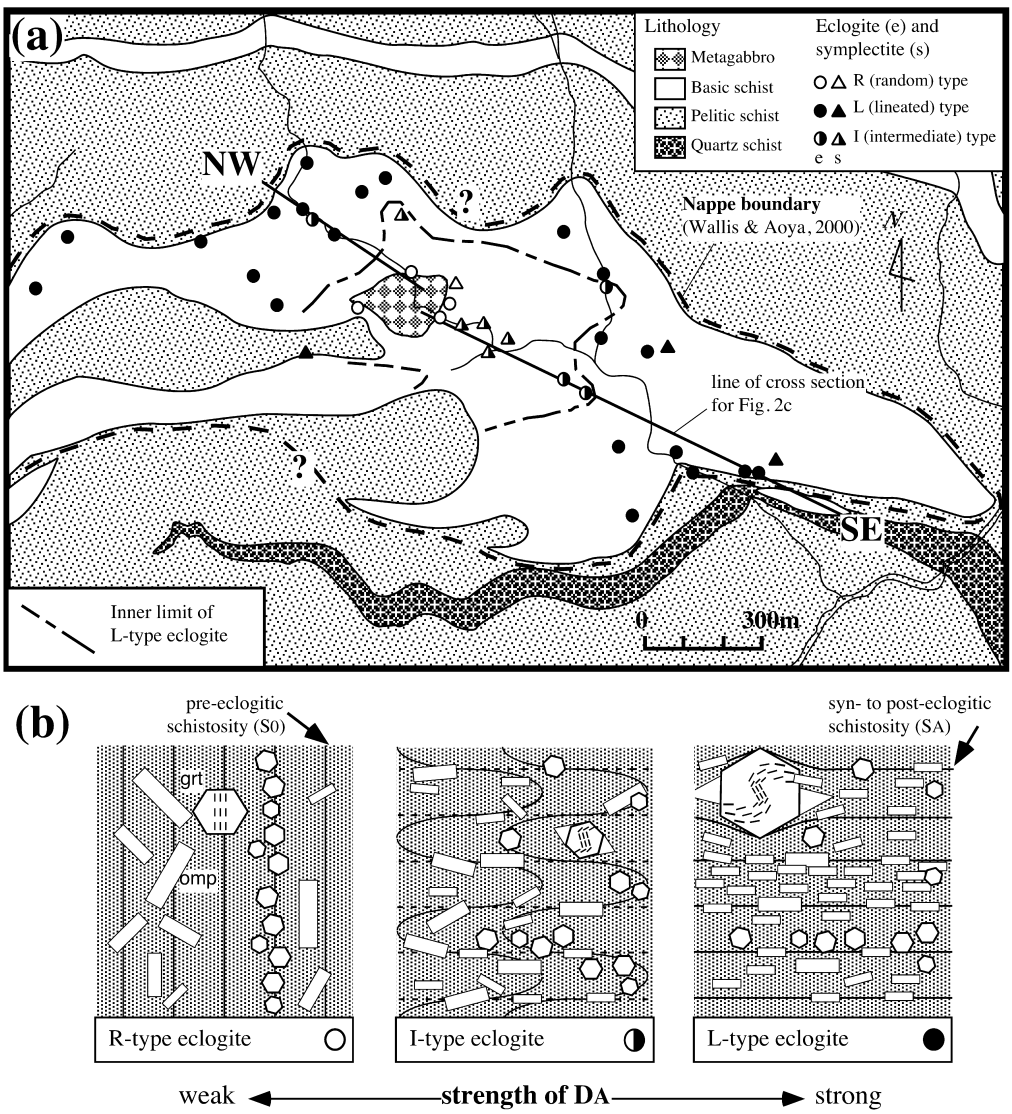


Fig. 3. (a) Geological map around the Seba eclogite unit showing localities of eclogite and albite–hornblende symplectite (pseudomorph after omphacite) in the Seba basic schist. R type = eclogite with randomly oriented omphacite; L type = eclogite with strong linear alignment of omphacite; I type = eclogite with intermediate texture between R and L types (see also (b)). The location of cross-sections for Fig. 2c and the inner limit of L-type eclogites are also shown. (b) Schematic illustrations showing microstructure of the three types of eclogite from the Seba basic schist. $S_A$ schistosity can be identified by the presence of I- or L-type microstructure.

coarse-grained and randomly oriented fabric (R type: R = random) to a fine-grained and strongly aligned fabric (L type: L = lineated) reflecting increasing strength of $D_A$ deformation (Aoya and Wallis, 1999; Fig. 3b). Documentation of the distribution of these three omphacite microstructures (R, L and I types: I = intermediate) in the Seba basic schist shows that the L type is restricted to the outermost part of the Seba basic schist while the R or I types occur in the more central part (Fig. 3a). This finding also shows that the effect of $D_A$ deformation is stronger in the outermost part of the Seba basic schist and weaker in the more central part.

Cross-sections clearly show that the Seba fold has a downward closure implying, therefore, that the perpendicular

Fig. 4. (a) Triangular plot showing chemical composition of garnet from the three localities, A, B and C, in Fig. 2c (modified from Aoya, 2001). All analysed garnet grains have a very similar limited range of chemical composition. (b) Photomicrograph of a garnet grain from locality B showing the presence of two distinct foliations within it. Long axis is 1 mm. This photo and Fig. 5b are from the same thin section. Abbreviations: grt = garnet; omp = omphacite; bar = barroisite; epi = epidote; qtz = quartz. (c) X-ray colour maps (for Mg, Fe, Ca and Mn) of garnet shown in (b). For all the elements, concentric zoning patterns with nearly hexagonal contours are preserved suggesting that growth of the whole garnet occurred progressively during a single phase of metamorphism.

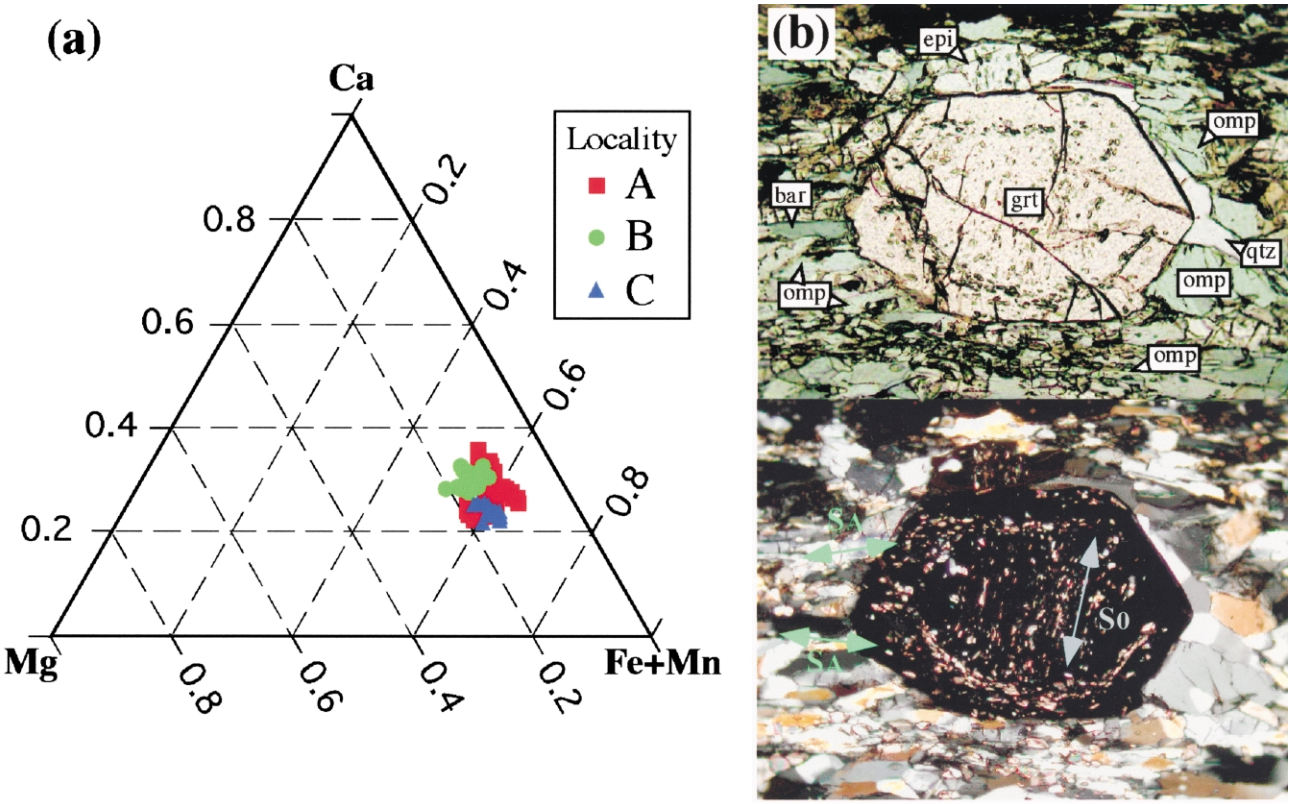
(a)
Ca
Mg
Fe+Mn
0.2
0.4
0.6
0.8
Locality
A
B
C
(b)
epi
omp
bar
grt
qtz
omp
omp
omp
Sa
So
Sa

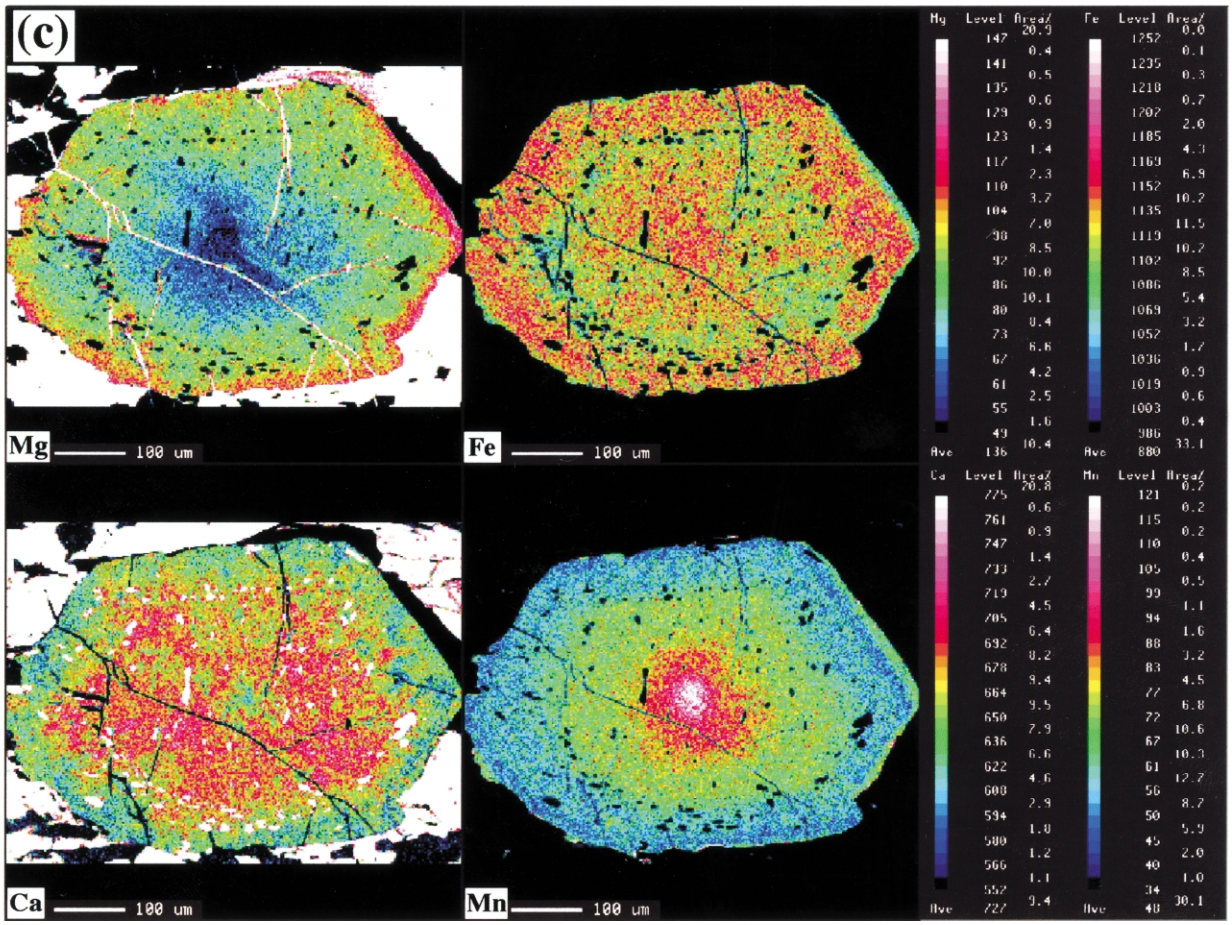
(c)
Mg
100 um
Fe
100 um
Ca
100 um
Mn
100 um

distance from the nappe boundary increases going from the marginal to the central parts of the Seba unit (Fig. 2c). The distribution of $F_A$ folds and omphacite microstructures in the Seba basic schist can, therefore, be interpreted as showing a gradient in the total $D_A$ strain decreasing away from the nappe boundary.

## 4. Time-dependent shear-zone widening from the nappe boundary

### 4.1. Synchronous growth of garnet in the Seba basic schist

This section focuses on the internal microstructures of garnet in eclogite samples taken from three spatially distinct localities adjacent to the cross-section (A, B and C in Fig. 2c). Aoya (2001) suggests that all garnet in the Seba basic schist formed primarily during a single eclogite-facies metamorphism. The main supporting evidence is: (i) all analysed garnet grains from the Seba basic schist eclogite have a very similar limited range of chemical composition; (ii) almost all analysed garnet grains from the Seba basic schist eclogite show a continuous chemical zoning lacking sudden jumps in chemical composition (the detrital garnet described by Wallis and Aoya (2000) is the only exception); and (iii) garnet in the Seba basic schist eclogite grew synchronously with omphacite that lacks clear chemical zoning. Chemical analyses of eclogitic garnet have been carried out at localities A, B and C and the results support their synchronous growth during a single phase of eclogite facies metamorphism (Fig. 4).

### 4.2. Locality A

For locality A, the main features of the internal microstructure of garnet are already described by Aoya (2001) as follows:

(i) Inclusion trails in the garnet show a sigmoidal curvature. In addition, fine-grained straight inclusion trails are also rarely observed in the core of the garnet. In this case, the garnet grains contain a composite inclusion trail that includes a straight segment in the core and a sigmoidally curved segment in the outer part (Fig. 5a).
(ii) The inclusion trails in the outermost rim of garnet are continuous with $S_A$ schistosity of the surrounding matrix (Fig. 5a), indicating that the outer part of garnet with sigmoidal-inclusion trails grew synchronously with $D_A$. The rare straight inclusion trails found in the garnet core can be interpreted as an older schistosity, $S_0$ (Figs. 2b and 3b), and growth of the garnet is likely to have been initiated during a non-deformational stage between $D_0$ and $D_A$.

Aoya (2001) refers to this type of garnet with composite inclusion trails as 'sickle garnet', because the shape traced by the inclusion trails resembles a sickle. The point is that sickles at locality A have very short or absent hafts: the core region with straight inclusion trails is very small or even lacking. This indicates that at locality A there was a relatively short growth period of garnet during a non deformational stage between $D_0$ and $D_A$ and $D_A$ deformation started shortly after the initiation of garnet growth.

### 4.3. Locality B

Through recent studies, it has become clear that garnet grains from locality B have the same type of inclusion-trail patterns as those from locality A (Fig. 5b). For example, the garnet grain of Fig. 5b clearly has a composite inclusion trail that includes a straight segment in the inner part and a sigmoidally curved segment in the outer part. This type of microstructure is common in locality B. Other grains in the same thin section (Fig. 4b) further confirm that these two sets of inclusion trails formed during two distinct deformation stages, $D_0$ and $D_A$. In the garnet of Fig. 4b, straight inclusion trails of the inner segment are clearly at a high angle to those of the outer segment. In addition, the arrangement of the outer inclusion trails, which are subparallel to surrounding $S_A$, form strain caps wrapping the inner segment with straight inclusion trails (Fig. 4b). The presence of this kind of microstructure clearly shows that the composite inclusion-trail patterns such as the one shown in Fig. 5b do not represent, for example, a small asymmetric fold statically overgrown by garnet. An additional point that needs to be emphasised is that the chemical zoning patterns of this garnet show nearly concentric contours and gradual changes from core to rim for all major components (Fig. 4c). This suggests that the garnet grew during a single phase of metamorphism without any dissolution event even between the microstructurally distinct inner and outer domains.

Grains of sickle garnet from both localities A and B, therefore, record the initiation of $D_A$ deformation during a single phase of growth. One important difference, however, is that the sickle garnet from locality B has relatively long

Fig. 5. Photomicrographs of garnet and omphacite in eclogite from the Seba basic schist. See text for detailed explanations. (a) Porphyroblastic garnet from locality A (Fig. 2c). Crossed nicols. Long axis is 3.4 mm. (b) Porphyroblastic garnet from locality B. Crossed nicols. Long axis is 1.4 mm. (c) Porphyroblastic garnet from locality C. Crossed nicols. Long axis is 2.8 mm. (d) Porphyroblastic omphacite from locality C. Open nicol. Long axis is 3.4 mm. (e) Schematic illustration showing the time-dependent evolution of microstructures of garnet from localities A, B and C. Time-dependent shear-zone widening from the nappe boundary can be discerned in the illustration. The same stage numbers (1)–(4) are used in the text.

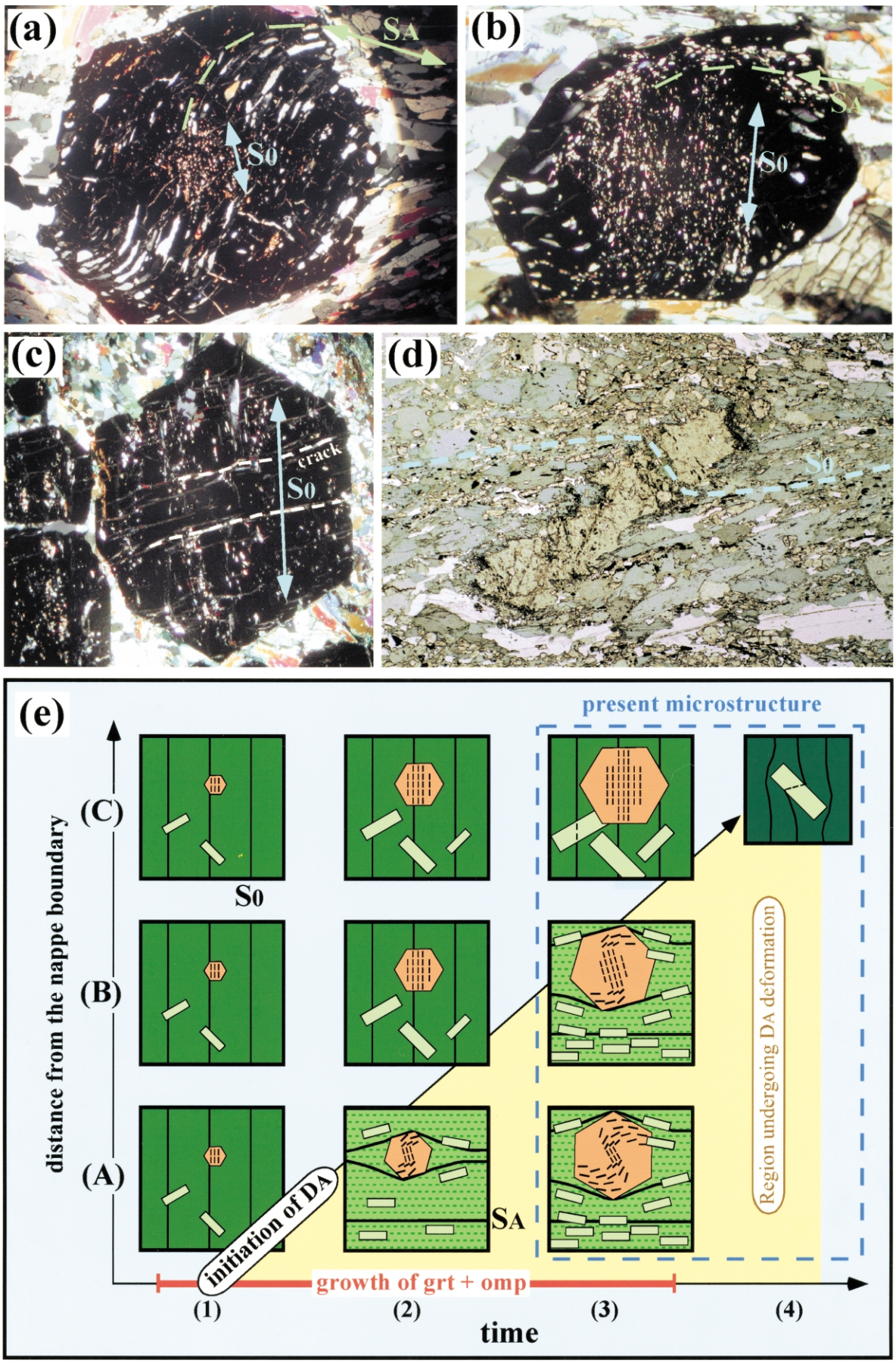
(a)
SA
S0
(b)
SA
S0
(c)
crack
S0
(d)
S0
(e)
present microstructure
(C)
(B)
(A)
S0
SA
distance from the nappe boundary
initiation of DA
growth of grt + omp
Region undergoing DA deformation
(1)
(2)
(3)
(4)
time

hafts and the blade region is limited to the outermost part (Figs. 4b and 5b). This indicates that at locality B the period of growth of garnet during the non-deformational stage between $D_0$ and $D_A$ was significantly longer than at locality A and that initiation of $D_A$ deformation occurred relatively later with respect to garnet growth.

### 4.4. Locality C

The broadening of the statically grown domain in garnet develops one stage further in moving from locality B to locality C: porphyroblastic garnet grains from locality C show only hafts with no blades (Fig. 5c;/ figure 6 in Takasu, 1984). In locality C the dominant schistosity in outcrop is not $S_A$ but $S_0$ (Figs. 2b and 3b), and the haft, or straight inclusion trail in garnet, lies parallel to the surrounding $S_0$. This indicates that growth of the whole of the garnet occurred during a non-deformational stage after $D_0$ without association of $D_A$ deformation. However, minor effects of $D_A$ deformation can also be observed in locality C. Omphacite grains from locality C commonly contain straight inclusion trails, $S_0$, as in the case of porphyroblastic garnet (Fig. 3b), and these inclusion trails are locally slightly rotated with respect to the external foliation associated with gentle $F_A$ folding (Fig. 5d). This indicates that at locality C $D_A$ deformation started after growth of garnet + omphacite although its effect is minor.

### 4.5. Summary: evolution of $D_A$ shear zone

Based on the assumption that growth of garnet at localities A, B and C occurred synchronously, a comprehensive growth history for the $D_A$ shear zone can be deduced as follows (Fig. 5e). (1) *Initial stage of garnet growth*. In all three localities, growth of garnet begins in a non-deformational stage before $D_A$. Garnet in all three localities overgrows a pre-existing $S_0$ schistosity. (2) *Early stage of garnet growth*. $D_A$ deformation starts shortly after the initiation of the growth of garnet, but at this stage is restricted to locality A. Non-coaxial $D_A$ deformation causes rotation of the garnet and the garnet at locality A begins to overgrow $S_A$ schistosity developing a sigmoidal internal fabric. Garnet at localities B and C also grows, but here $S_0$ schistosity remains the only included fabric. (3) *Later stages of garnet growth*. $D_A$ deformation also starts at locality B and garnet at this locality begins to undergo syn-growth rotation caused by non-coaxial $D_A$ deformation. Garnet at locality A continues to grow associated with rotation, while garnet at locality C continues to grow under non-deformational conditions. (4) *Post-eclogitic stage*. Although garnet and omphacite in locality C completely overgrow the $S_0$ associated with no deformation, $D_A$ deformation also starts to affect locality C after growth of garnet + omphacite stopped.

The localities A, B and C are arranged in order of increasing distance from the nappe boundary (Fig. 2c) implying the above sequence reflects time-dependent shear-zone widening from the nappe boundary (Fig. 5e). During stage (2), the $D_A$ shear zone that nucleated at the nappe boundary was relatively thin encompassing only locality A. By stage (3), however, the $D_A$ shear zone had grown and encompassed an area extending from nappe boundary and including locality B. Ultimately, the effect of $D_A$ deformation reaches locality C, although here its effect is minor.

## 5. Implications

### 5.1. Shear-zone widening and reconstruction of geological history

The observations summarised above indicate that there was progressive time-dependent shear-zone widening from the nappe boundary of the Seba eclogite unit. In this type of shear zone, it is easier to deform undeformed material at the zone margins than to continue deforming the already deformed material near the core zone. It can, therefore, be said that the Seba basic schist, dominantly composed of epidote amphibolite, behaved as a strain-hardening material during $D_A$ deformation. The strain hardening, or shear-zone widening, seen in the Seba basic schist raises an important general problem for geologists. We often discuss the evolution of a given unit assuming that two or more geologic features observed in different outcrops can be regarded as features representative of different moments in the overall evolution of the unit. In the case of shear-zone widening, however, it is clear that this assumption is misleading (e.g. Means, 1995). In the Seba basic schist, it will lead to confusion if one tries to discuss the microstructural evolution of eclogite simply by ordering the present internal microstructures of garnet from the three localities (Fig. 5a–c). It is probable that the only way to overcome this problem is to discuss the chronological order of geologic events not for a geologic unit but for a single outcrop. For example, discussing the chronological relationship between growth of garnet and $D_A$ deformation for the Seba unit may have little meaning because growth of garnet is mainly syn-$D_A$ at locality A and pre-$D_A$ at locality C (Fig. 5a and c). In this case, the question of whether the growth of garnet is synchronous with or predates $D_A$ cannot be satisfactorily answered for the Seba unit as a whole, but only for a single outcrop.

### 5.2. Deformation stages and nappe tectonics

Aoya (2001) concludes that the exhumation-related $D_A$ of the Seba basic schist and subduction-related $D_r$ of the surrounding non-eclogitic schist (e.g. Wallis, 1998) occurred synchronously along the active subduction boundary between them, which coincides with the proposed boundary between the eclogite and Besshi nappes. In addition this contribution has revealed that the nappe

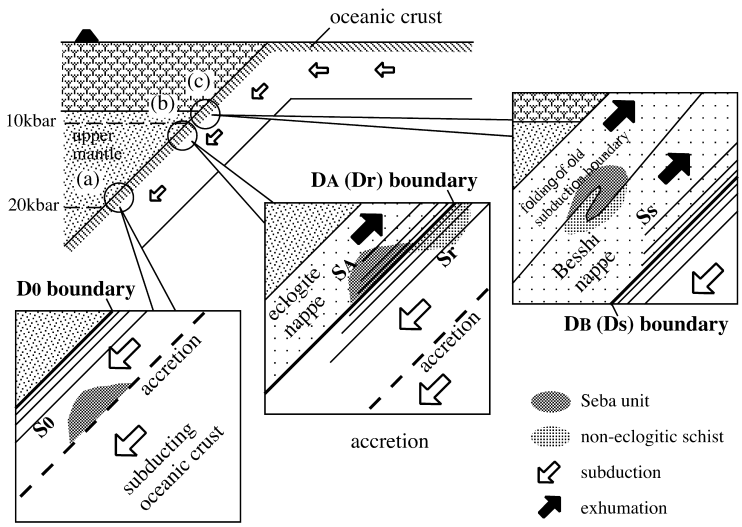


Fig. 6. Schematic illustration showing relationship between nappe tectonics and regional deformation stages in the Sambagawa belt based on the proposed model. (a) Initial subduction and accretion of the eclogite nappe. $D_O$ is related to the initial subduction boundary. (b) Exhumation of the eclogite nappe and subduction of the Besshi nappe. $D_A$ ($D_r$) is related to the subduction boundary generated beneath the eclogite nappe. (c) Exhumation of the eclogite and Besshi nappes with subduction of the Oboke nappe. $D_S$ ($D_B$) is related to the subduction boundary generated beneath the Besshi nappe.

boundary behaved as a core zone with strength of $D_A$ decreasing away from it and with $D_A$ deformation propagating away from it. These features indicate that deformation during the $D_A$ (or $D_r$ in the Besshi nappe) phase is strongly controlled by the nappe boundary, and further suggest that if a new subduction boundary is formed due to the accretion of a thick sheet, a new stage of deformation will form, propagating away from the new subduction boundary. Each phase of penetrative deformation in a subduction zone may, therefore, represent deformation along a particular subduction boundary. Application of this model to the nappe tectonics of the Sambagawa belt is summarised in Fig. 6. The eclogite nappe includes a large peridotite mass (Higashi-Akaishi mass; Fig. 1) and can be considered to have subducted at least in part in direct contact with the mantle. $D_0$, the subduction-related deformation stage of the eclogite nappe (Aoya, 2001) can, therefore, be regarded as having occurred along the initial subduction boundary (Fig. 6a). $D_A$ of the eclogite nappe and $D_r$ of the Besshi nappe have been shown to be related to the subduction boundary generated after the accretion of the eclogite nappe (Aoya, 2001; Fig. 6b). The main deformation of the Besshi nappe, $D_S$ (e.g. Wallis, 1998), which corresponds to $D_B$ of the eclogite nappe (Aoya, 2001; Fig. 3b), can likewise be related to the subduction boundary generated after the accretion of Besshi nappe (Fig. 6c). Using this model, the significance of the main deformation stages in the Sambagawa belt can clearly be explained in terms of large-scale nappe tectonics.

When dealing with the tectonic evolution of metamorphic belts, it is common to find a non-deformational stage between two distinct deformational stages (e.g. Passchier and Trouw, 1996) and, in many cases, the reason for the existence of these non-deformational stages is not well explained. In the case of the present model, however, the reason is clear. The length of the non-deformational stage before a particular deformation stage differs depending on the distance from its related nappe boundary. At a locality immediately adjacent to the nappe boundary, the non-deformational stage before the boundary-related deformation will be nearly absent. As the distance from the nappe boundary becomes larger, the onset of the deformation is delayed resulting in a longer non-deformational period. The present kind of study can be expanded to test the model proposed here. The model predicts that the boundary between the Besshi nappe and the Oboke nappe behaved as a core zone for $D_S$ deformation (Fig. 6c). If the model is correct, the length of the non-deformational stage before $D_S$ should vary depending on the distance from the nappe boundary. Albite porphyroblasts in the Besshi nappe generally have a composite internal microstructure with a straight segment in the core and a sigmoidally curved segment in the outer part (Wallis et al., 1992; Wallis, 1998). In addition, albite porphyroblasts that grew entirely during $D_S$ (e.g. Wallis, 1990) and entirely unrelated to deformation (Aoya, 2002) are both present. The spatial distribution of these different microstructures of albite porphyroblasts in relation to the boundary between the Besshi and Oboke nappes is a subject for future study.

## Acknowledgements

We are very grateful to Masaki Enami and Yoko Yasutaka for their help with the X-ray colour mapping of garnet. We thank Kazuhiko Ishii and John Miller for their constructive comments on this manuscript. M.A. acknowledges the

financial support of a JSPS Research Fellowship for Young Scientists.

## References

Aoya, M., 2001. P–T–D path of eclogite from the Sambagawa belt deduced from combination of petrological and microstructural analyses. Journal of Petrology 42, 1225–1248.

Aoya, M., 2002. Structural position of the Seba eclogite unit in the Sambagawa belt: supporting evidence for an eclogite nappe. The Island Arc 11, 91–110.

Aoya, M., Wallis, S.R., 1999. Structural and microstructural constraints on the mechanism of eclogite formation in the Sambagawa belt, SW Japan. Journal of Structural Geology 21, 1561–1573.

Banno, S., Nakajima, T., 1992. Metamorphic belts of Japanese islands. Annual Review of Earth and Planetary Science 20, 159–179.

Burg, J.-P., Chaudry, M.N., Ghanzanfar, M., Anckiewicz, R., Spencer, D., 1992. Structural evidence for back-sliding of the Kohistan Arc on the collisional system of northwest Pakistan. Geology 24, 739–742.

Enami, M., 1996. Petrology of kyanite-bearing tectonic blocks in the Sanbagawa metamorphic belt of the Bessi area, central Shikoku, Japan. In: Shimamoto, T., Hayasaka, Y., Shiota, T., Oda, M., Takeshita, T., Yokoyama, S., Ohtomo, Y. (Eds.), Tectonics and Metamorphism (Memorial Volume for Prof. I. Hara), Hiroshima University Press, pp. 47–55, (in Japanese with English abstract).

Froitzheim, N., 1992. Formation of recumbent folds during synorogenic crustal extension (Austroalpine nappes, Switzerland). Geology 20, 923–926.

Higashino, T., 1990. The higher grade metamorphic zonation of the Sambagawa metamorphic belt in central Shikoku, Japan. Journal of Metamorphic Geology 8, 413–423.

Means, W.D., 1995. Shear zone and rock history. Tectonophysics 257, 157–160.

Passchier, C.W., Trouw, R.A.J., 1996. Microtectonics, Springer, Berlin.

Platt, J.P., Soto, J.-I., Whitehouse, M.J., Hurford, A.J., Kelley, S.P., 1998. Thermal evolution, rate of exhumation, and tectonic significance of metamorphic rocks from the floor of the Alboran extensional basin, western Mediterranean. Tectonics 17, 671–689.

Quinquis, H., Audren, Cl, Brun, J.P., Cobbold, P.R., 1978. Intensive progressive shear in Ile de Groix blueschists and compatibility with subduction or obduction. Nature 273, 43–45.

Roeder, D.H., 1973. Subduction and orogeny. Journal of Geophysical Research 78, 5005–5024.

Takasu, A., 1984. Prograde and retrograde eclogite in the Sambagawa metamorphic belt, Besshi district, Japan. Journal of Petrology 25, 614–643.

Takasu, A., 1989. P–T histories of peridotite and amphibolite tectonic blocks in the Sambagawa metamorphic belt, Japan. In: Daly, J.S., Cliff, R.A., Yardley, B.W.D. (Eds.), Evolution of Metamorphic Belts. Geological Society Special Publication 43, pp. 533–538.

Takasu, A., Wallis, S.R., Banno, S., Dallmeyer, R.D., 1994. Evolution of the Sambagawa metamorphic belt. Lithos 33, 119–134.

Wallis, S.R., 1990. The timing of folding and stretching in the Sambagawa belt: the Asemigawa region, central Shikoku. Journal of Geological Society of Japan 96, 345–352.

Wallis, S.R., 1998. Exhuming the Sanbagawa metamorphic belt. the importance of tectonic discontinuities. Journal of Metamorphic Geology 16, 83–95.

Wallis, S.R., Aoya, M., 2000. A re-evaluation of eclogite facies metamorphism in SW Japan: proposal for an eclogite nappe. Journal of Metamorphic Geology 18, 653–664.

Wallis, S.R., Banno, S., Radvanec, M., 1992. Kinematics, structure and relationship to metamorphism of the east–west flow in the Sambagawa belt, southwest Japan. The Island Arc 1, 176–185.